A Screen for Conditional Growth Suppressor Genes Identifies the *Drosophila* Homolog of HD-PTP as a Regulator of the Oncoprotein Yorkie

M. Melissa Gilbert,[1,*] Marla Tipping,[2] Alexey Veraksa,[2] and Kenneth H. Moberg[1,*]
[1]Department of Cell Biology, Emory University School of Medicine, Atlanta, GA 30322, USA
[2]Department of Biology, University of Massachusetts Boston, Boston, MA 02125, USA
*Correspondence: mgilbert@cellbio.emory.edu (M.M.G.), kmoberg@emory.edu (K.H.M.)
DOI 10.1016/j.devcel.2011.04.012

SUMMARY

Mammalian cancers depend on "multiple hits," some of which promote growth and some of which block apoptosis. We screened for mutations that require a synergistic block in apoptosis to promote tissue overgrowth and identified *myopic* (*mop*), the *Drosophila* homolog of the candidate tumor-suppressor and endosomal regulator His-domain protein tyrosine phosphatase (HD-PTP). We find that Myopic regulates the Salvador/Warts/Hippo (SWH) tumor suppressor pathway: Myopic PPxY motifs bind conserved residues in the WW domains of the transcriptional coactivator Yorkie, and Myopic colocalizes with Yorkie at endosomes. Myopic controls Yorkie endosomal association and protein levels, ultimately influencing expression of some Yorkie target genes. However, the antiapoptotic gene *diap1* is not affected, which may explain the conditional nature of the *myopic* growth phenotype. These data establish Myopic as a Yorkie regulator and implicate Myopic-dependent association of Yorkie with endosomal compartments as a regulatory step in nuclear outputs of the SWH pathway.

INTRODUCTION

The link between unrestrained proliferation and the evasion of apoptosis in vertebrate tumors is well established (e.g., Evan and Vousden, 2001). Many growth-promoting lesions such as amplification of *c-Myc* or the loss of *Rb* trigger compensatory apoptosis, which must then be overcome by antiapoptotic lesions in order for tumorigenesis to proceed. Many of the molecular mechanisms that drive tumorigenesis are conserved in *Drosophila melanogaster*, and in recent years, *Drosophila* has proven itself amenable to the study of cooperating mutations that drive tumor progression and metastasis (Brumby and Richardson, 2005; Chi et al., 2010; Pagliarini and Xu, 2003; Wu et al., 2010). In some cases, this cooperativity has been shown to arise from synergistic effects on cell proliferation and death pathways (Asano et al., 1996; Nicholson et al., 2009; Pellock et al., 2007; Staehling-Hampton et al., 1999), yet the extent to

which compensatory apoptosis has hindered the identification of a conditional class of growth suppressor genes in *Drosophila* has not been comprehensively examined.

The conserved Salvador/Warts/Hippo (SWH) pathway controls a transcriptional program that includes both progrowth and antiapoptotic targets (Halder and Johnson, 2011; Pan, 2010). Pathway components include the protocadherin Fat, the apical membrane determinant Crumbs (Crb), and the FERM-domain proteins Expanded (Ex) and Merlin (Mer) (Bennett and Harvey, 2006; Chen et al., 2010; Cho et al., 2006; Grzeschik et al., 2010; Hamaratoglu et al., 2006; Ling et al., 2010; Robinson et al., 2010; Silva et al., 2006; Willecke et al., 2006). These factors regulate a core serine/threonine kinase cassette consisting of the Ste20-like kinase Hippo (Hpo) (Harvey et al., 2003; Jia et al., 2003; Pantalacci et al., 2003; Udan et al., 2003; Wu et al., 2003), which acts together with the scaffolding protein Salvador (Sav) (Kango-Singh et al., 2002; Tapon et al., 2002) to phosphorylate the NDR family kinase Warts (Wts) (Justice et al., 1995; Xu et al., 1995). Wts then (Lai et al., 2005) phosphorylates the cotranscriptional activator Yorkie (Yki) on sites including Ser168 (S168) (Dong et al., 2007; Huang et al., 2005). This modification anchors Yki in the cytoplasm by recruiting 14-3-3 proteins (Oh and Irvine, 2008). In the absence of SWH signaling, Yki shuttles into the nucleus and, together with sequence-specific DNA binding factors (Goulev et al., 2008; Peng et al., 2009; Wu et al., 2008; Zhang et al., 2008; Zhao et al., 2008), activates a transcriptional program including the progrowth microRNA *bantam*, the prodivision gene *cyclin E* (*cycE*), the antiapoptotic gene *diap1*, and the upstream regulators *ex* and *mer*.

The SWH pathway has potent antigrowth activity (for review, see Pan, 2010; Zhao et al., 2010), and multiple mechanisms exist to limit Yki activity in developing tissues. While S168 is critical for Yki:14-3-3 binding, Wts phosphorylation of S111 and S250 also contribute to Yki inhibition (Oh and Irvine, 2009; Ren et al., 2010). Yki is directly inhibited in a phosphorylation-independent manner via interactions between two WW domains within Yki that are bound by PPxY sequence motifs in Hpo, Wts, and Ex (Badouel et al., 2009; Oh et al., 2009). Mammalian cells have additional regulatory mechanisms to control activity of the Yki homolog Yes-associated protein (YAP). YAP is tyrosine phosphorylated by c-Src/Yes kinases, which modulates the ability of YAP to recruit the Runx2 protein and control osteoblast differentiation (Zaidi et al., 2004). DNA damage triggers the c-Abl kinase to phosphorylate YAP on Y357, and this may bias YAP toward the promoters of apoptotic genes over growth-arrest genes (Levy

A
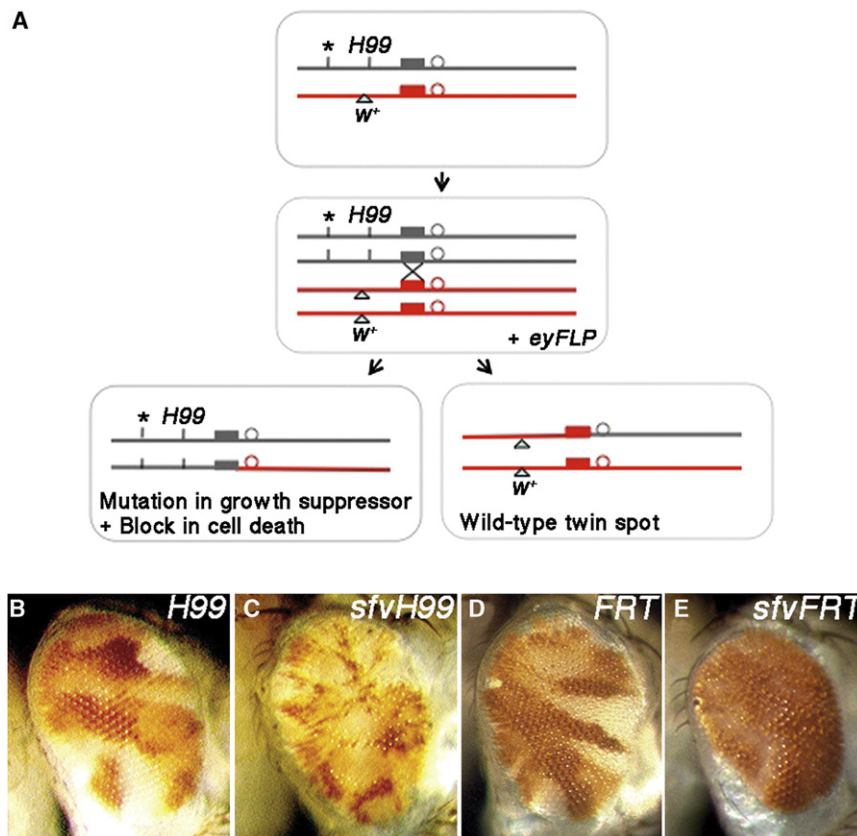
Figure 1. An *eyFLP* Mosaic Screen for Conditional Growth Suppressors

(A) Clones of cells carrying EMS-induced mutations (*) in the background of the *H99,FRT80B* chromosome were generated using the *eyFLP* transgene. Homozygous **H99,FRT* mutant cells are marked by the absence of the *P[m−w+]* transgene, and wild-type twin spots are marked by the presence of *P[m−w+]*.

(B–E) Representative images of *H99* alone (B), *sfvH99* (C), control *FRT80B* (D), and *sfvFRT80B* (E) mosaic adult eyes.

complexes as a SWH regulatory mechanism in developing tissues.

RESULTS

slaughterhouse-five Alleles Produce Conditional Tissue Overgrowth

We designed and implemented a screen for survival-dependent growth suppressor genes on *Drosophila* chromosome 3L. The screen used FLP recombinase driven by the promoter of the *eyeless* (*ey*) gene (Newsome et al., 2000) to produce a mixture of mutant clones (unpigmented) and wild-type twin spots (pigmented red) in the adult eye (Figure 1A). To block cell death in mutant clones, mutagenesis was carried out using a parental *FRT* chromosome carrying the genomic deletion *H99*, which removes genes required for virtually all developmentally programmed cell death (White et al., 1994). *H99* mutant clones display a block in developmental apoptosis in the pupal retina (30 hr after puparium formation [APF]) (see Figures S1A and S1A′ available online) and exhibit minimal phenotypes in the adult eye (Figures 1B versus 1D). We used this background to screen for recessive mutations that could synergize with *H99* to confer a growth advantage and identified a recessive-lethal complementation group, which we named *slaughterhouse-five* (*sfv*), consisting of two alleles (*F2.6.3* and *F2.6.11*) that exhibited a clonal growth advantage in the adult eye (Figure 1C) relative to an *H99* control. Experiments were carried out with the *sfv³* allele (*F2.6.3*) unless otherwise indicated. To test the survival-dependent nature of the *sfv* phenotype, the *H99* deletion was removed. Adult *sfv* mosaic eyes are small and rough and contain little to no *sfv* mutant tissue (Figure 1E). Clones of *sfv* mutant cells in the larval eye disc contain elevated levels of cleaved caspase-3 (C3) (Figures S1B and S1B′), indicating they are normally eliminated by apoptosis. Thus the overgrowth of *sfv* mutant cells is conditional on a synergistic block in cell death provided by the *H99* deletion.

sfv Is Allelic to *myopic*, the *Drosophila* Homolog of HD-PTP

The *sfv* lesions were mapped by deficiency mapping and candidate gene sequencing. This identified a nonsense mutation in the seventh exon of the gene *CG9311* on the *sfv³* chromosome. The

et al., 2008; Strano et al., 2005). This complexity indicates that mutations in peripheral SWH pathway components may selectively affect the transcriptional specificity of nuclear Yki.

Here, we apply a genetic approach to identify conditional growth suppressor mutants and identify Myopic (Mop) as a protein that physically interacts with Yki and restricts its activity. *mop* is a homolog of human His-domain protein tyrosine phosphatase gene (*HD-PTP* or *PTPN23*) (Toyooka et al., 2000), which is located in a region of the genome frequently deleted in cancers (Braga et al., 2002; Kok et al., 1997; Szeles et al., 1997). Mop and HD-PTP proteins contain an amino-terminal Bro1 domain and a carboxy-terminal domain with sequence homology to protein tyrosine phosphatase (PTPase) domains. HD-PTP interacts with endosomal proteins such as CHMP4b via the Bro1 domain and interacts with the ESCRT-1 component Tsg101 via sites outside the Bro1 domain (Doyotte et al., 2008; Ichioka et al., 2007; Kim et al., 2005; Miura et al., 2008; Odorizzi et al., 2003).

We find that cells lacking Mop display overgrowth phenotypes only in the context of a block in cell death. This growth is accompanied by upregulation of a subset of Yki transcriptional targets but not the antiapoptotic gene *diap1*. *mop* interacts genetically with *yki* and acts downstream of *wts*, but at the level of *ex* and *yki*. Mop protein colocalizes with Yki in endosomes and physically interacts with Yki via PPxY motifs in Mop and WW domains in Yki. Moreover, loss of *mop* shifts the endosomal localization of endogenous Yki and elevates Yki protein levels. These data identify Mop as an inhibitor of Yki in developing tissues and implicate Mop-dependent control of Yki-containing endosomal

CG9311 gene corresponds to *mop*, which encodes the *Drosophila* homolog of vertebrate HD-PTP. The *sfv³* mutation truncates Mop within its C-terminal region, just prior to the PTPase catalytic region (Figure S1H). The lesion in the *sfv¹¹* allele was not identified, but staining with an anti-Mop antibody shows reduced Mop protein levels in both *sfv³H99* and *sfv¹¹H99* eye clones (Figures S1C and S1C′; data not shown), indicating that both *sfv* alleles reduce Mop expression. The *sfv³* and *sfv¹¹* alleles fail to complement existing *mop* alleles (data not shown) and will be referred to as *mop^sfv3* and *mop^sfv11*.

Mop/HD-PTP is a conserved endosomal regulatory protein that contains an N-terminal Bro1 domain and a C-terminal predicted PTPase domain. The PTPase domain lacks activity in vitro due to an amino acid change in the phosphate-binding loop that diverges from all other active PTPases (Gingras et al., 2009), and this change is conserved in Mop. The Mop Bro1 domain is required to promote the endocytic trafficking and activity of the EGF and Toll receptors (Huang et al., 2010; Miura et al., 2008) and defects in differentiation of Elav-positive neurons within *mop* eye clones have been attributed to a defect in EGF signaling (Miura et al., 2008). However, some Elav-positive cells remain in *mop^sfvH99* clones (Figures S1D and S1E), and the R2/R5 photoreceptor marker Rough is increased in *mop^sfvH99* clones relative to *mop^sfv* clones (Figures S1F and S1G). Thus, the lack of photoreceptors in *mop* mutant clones may be due to excess apoptosis and impaired EGF-dependent photoreceptor recruitment.

mop Mutations Collaborate with a Block in Cell Death to Elicit Organ Overgrowth

Genetic manipulations that simultaneously increase proliferation and reduce apoptosis often increase organ size. To test the effect of the *mop^sfvH99* genotype on organ size, the recessive cell-lethal *Minute* technique was used to generate heads composed entirely of *mop^sfvH99* cells (*mop^sfvH99/M(3)*). These animals die at the pharate adult stage with extra folds of head cuticle relative to control heads and eyes that are constricted at their margins and protrude from the head (Figures 2A–2D) and contain enlarged facets (data not shown). Generation of *mop^sfvH99* clones throughout the body produced outgrowths in the adult thorax (Figures 2E and 2F) and increased haltere size (Figures 2G and 2H) relative to *H99* controls. Thus, combined loss of Mop and the *H99* proapoptotic genes increases the growth of multiple types of epithelia.

mop Loss Increases Cell Proliferation Rates and Inhibits Cell-Cycle Exit

The synergy between *mop^sfv* and *H99* alleles indicates that *mop* loss may increase cell number, conditional on a block in apoptosis. Staining with anti-Discs large (Dlg) to mark apical cell profiles reveals excess interommatidial cells (IOCs) in *mop^sfvH99* pupal eye clones relative to *H99* mutant clones (Figures 3A and 3B). Patterning defects are also evident within *mop^sfvH99* mutant pupal clones, which may be a consequence of additional roles for Mop in cell fate pathways (e.g., Miura et al., 2008). Scattered ectopic S phase cells appear among *mop^sfvH99* mutant cells posterior to the second mitotic wave (SMW) (Figures 3C–3F), which normally marks the point at which cells become postmitotic (Wolff and Ready, 1993); this pheno-
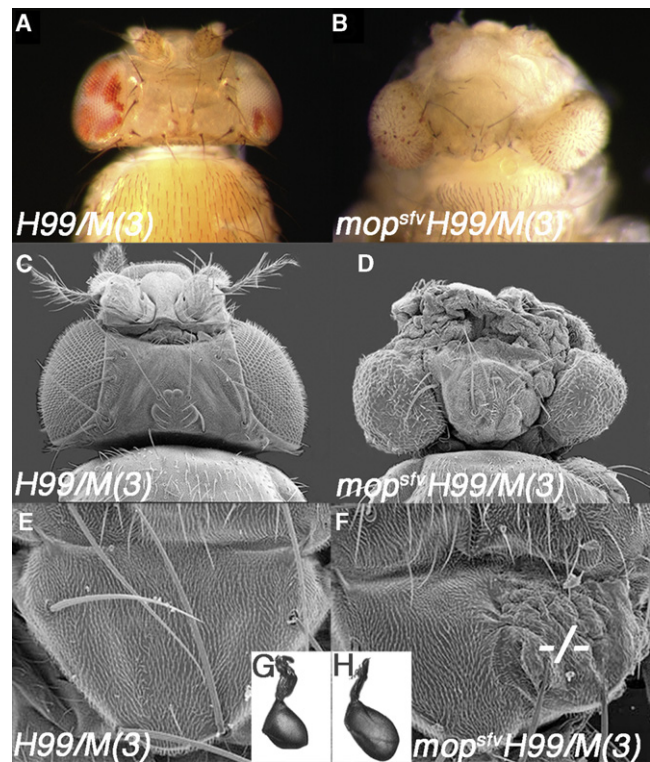
Figure 2. *mop* **Loss Cooperates with a Block in Death to Increase Organ Size**
(A and B) Bright-field images of control *H99/M(3)* (A) and *mop^sfvH99/M(3)* (B) eyes/heads.
(C and D) Scanning electron micrographs (SEM) of control *H99/M(3)* (C) and *mop^sfvH99/M(3)* (D) eyes/heads.
(E and F) SEM of *H99* (E) and *mop^sfvH99* (F) clones in adult thoraces. *mop^sfvH99* mutant tissue is marked by dashes (−/−).
(G and H) Images of mosaic *H99* (G) and *mop^sfvH99* (H) halteres.

type is not evident in *H99* control clones (Figure 3D). *mop^sfvH99* mutant eye clones also show a perdurance of cyclin A and, to a lesser extent, cyclin E, posterior to the morphogenetic furrow (MF) (Figures 3G–3L). To test whether *mop* limits cell division, the rate of clonal expansion of *H99* and *mop^sfvH99* clones were analyzed in the wing disc epithelium at fixed time points after clonal induction. *mop^sfvH99* clones are consistently larger and contain more cells than wild-type "twin spots" or control clones homozygous for the *H99* deletion (Figures 3N and 3O); the boundaries of *mop^sfvH99* clones tend to be regular (Figure 3M, top left panel), suggesting that *mop* loss may affect cell adhesion. Fluorescence-activated cell sorting (FACS) analysis of *mop^sfvH99* and *H99* wing disc cells relative to a control *ubi > GFP* chromosome indicates that *mop^sfvH99* cells have a DNA-content profile and size similar to *H99* control cells (Figure 3M). Thus, although *mop^sfvH99* mutant cells proliferate more rapidly than control cells, this is not accompanied by an overall shift in cell-cycle phasing.

mop Promotes SWH Signaling and Functions Downstream of the Core SWH Kinase Cassette

The *mop^sfvH99* mutant growth phenotypes resemble those associated with Sav/Wts/Hpo (SWH) pathway mutants (for
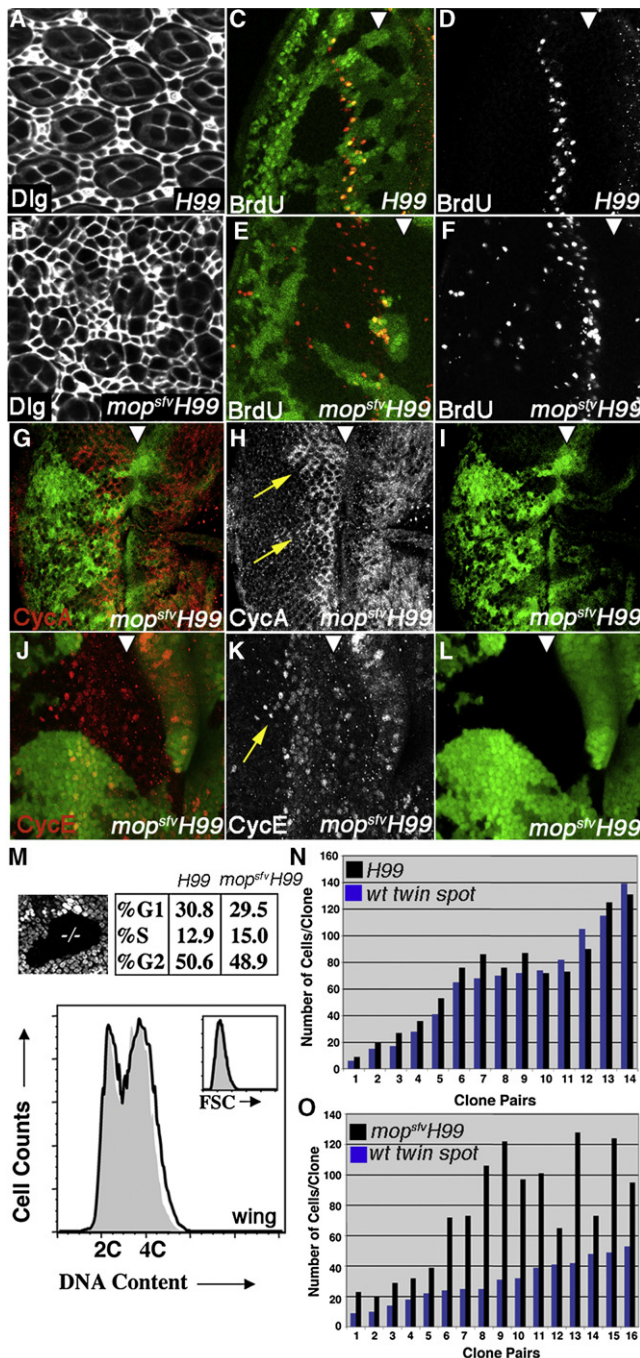
Figure 3. *mop* Limits Cell Division

(A and B) Confocal images of *H99* (A) and *mop^sfvH99* (B) pupal eye clones (40 hr APF) stained with anti-Dlg.

(C–L) Images of *H99* (C and D) or *mop^sfvH99* (E–L) eye clones marked by the absence of GFP (green) and stained for BrdU incorporation (C–F), Cyclin A (G–I), or Cyclin E (J–L). The morphogenetic furrow (MF) is marked by an arrowhead in (C)–(L). Yellow arrows in (H) denote perdurance of Cyclin A posterior to the MF. Yellow arrow in (K) denotes perdurance of Cyclin E in basal nuclei posterior to the MF.

(M) Confocal image of a *mop^sfvH99* mutant wing clone (black, −/−) and its wild-type twin spot (white) and corresponding flow cytometric analysis of DNA content and cell size ("FSC"; see inset) in *H99/M(3)* (gray fill) and *mop^sfvH99/M(3)* (black line) early third instar wing discs.

review, see Pan, 2010). We therefore tested the effect of *mop* alleles on expression of SWH target genes and proteins. Expression of the *ex-lacZ* transcriptional reporter (*ex-Z*) is upregulated in apically located *mop^sfvH99* mutant cells posterior to the MF (Figures 4A and 4A′); this effect is most apparent in transverse sections of peripodial cells (Figures 4B and 4B′) but is also detectable by qRT-PCR analysis of *ex* mRNA in intact discs. Ex protein levels are increased in tangential (Figures 4C and 4C′) and transverse (Figures 4D and 4D′) sections of *mop^sfvH99* clones. Control *H99* clones have no effect on *ex-Z* or Ex (Figures S2A, S2A′, S2B, S2B′, S2C, and S2D). *mop^sfvH99* mutant disc cells accumulate the apical membrane protein Crb (Figures 4E and 4F), which occurs in *wts* mutant cells via a Yki-dependent mechanism (Genevet et al., 2009; Hamaratoglu et al., 2009). Wg protein accumulates in *mop^sfvH99* clones located in the hinge and notum regions of the larval wing (Figures 4G and 4H), which also occurs in some SWH mutants (Cho et al., 2006; Hamaratoglu et al., 2006; Maitra et al., 2006; Pellock et al., 2007). Expression of a *mop* inverted repeat (*UAS-mop^IR*) transgene in the posterior wing disc reduces expression of the *bantam-GFP* sensor (*ban-GFP*) (Figures 4I and 4J), indicating that levels of the *ban* miRNA (Oh and Irvine, 2011) are elevated in Mop-depleted cells. Parallel analysis of the effect of *mop^IR* on epitope-tagged Yki (Yki:V5) (Oh and Irvine, 2009) shows that knockdown of *mop* causes Yki:V5 to accumulate in the cell cytoplasm (Figures S2I and S2J). Consistent with an inhibitory role for Mop in the SWH pathway, heterozygosity for a *yki* mutant allele efficiently suppressed the overgrowth of *mop^sfvH99/M(3)* eyes and heads (Figures 4K and 4L). Thus, although Mop loss does not stabilize Yki in the nucleus, its effect on the expression of SWH targets and its genetic dependence on a diploid dose of *yki* argues that the *mop^sfvH99* growth phenotype is mediated at least in part by elevated Yki activity.

Genetic analysis was used to place *mop* into a functional hierarchy with other SWH pathway genes. Expression of Wts suppresses disc growth (Lai et al., 2005; Wei et al., 2007), yet overexpression of Wts in the *mop^sfvH99/M(3)* background has no effect on the size or morphology of pharate adult heads (Figures 4M and 4N). By contrast expression of full-length Ex (either *UAS-Ex* or *UAS-Ex:GFP*), which can act downstream of Wts via direct binding to Yki (Badouel et al., 2009), suppresses the size of *mop^sfvH99/M(3)* heads (Figures 4O and 4P). The C terminus of Ex (CT:GFP), which contains PPxY motifs that bind Yki, is a more potent suppressor of the *mop^sfvH99/M(3)* growth phenotype than full-length Ex:GFP, while the control linker domain of Ex (linker:GFP) has no effect on *mop^sfvH99/M(3)* heads (Figures S2K–S2P). CT:GFP had only a slight effect on the size of control heads, indicating that loss of *mop* sensitizes cells to elevated levels of Ex. To test synergy between Mop and Ex loss, these factors were knocked down individually or in combination in the developing eye using *UAS-ex^IR* and *UAS-mop^IR* transgenes. While *ex^IR* or *mop^IR* individually produce a mild increase in IOCs in the pupal eye, combined expression of both enhances the IOC phenotype (Figures 4Q–4T). This genetic interaction between Mop and Ex in control of IOC numbers

(N and O) Cell number in individual *H99* (N) or *mop^sfvH99* (O) clone:twin spot pairs. Data are arranged in order of increasing clone size. Variation in *mop^sfvH99* cell counts is due to position-specific effects in the wing.
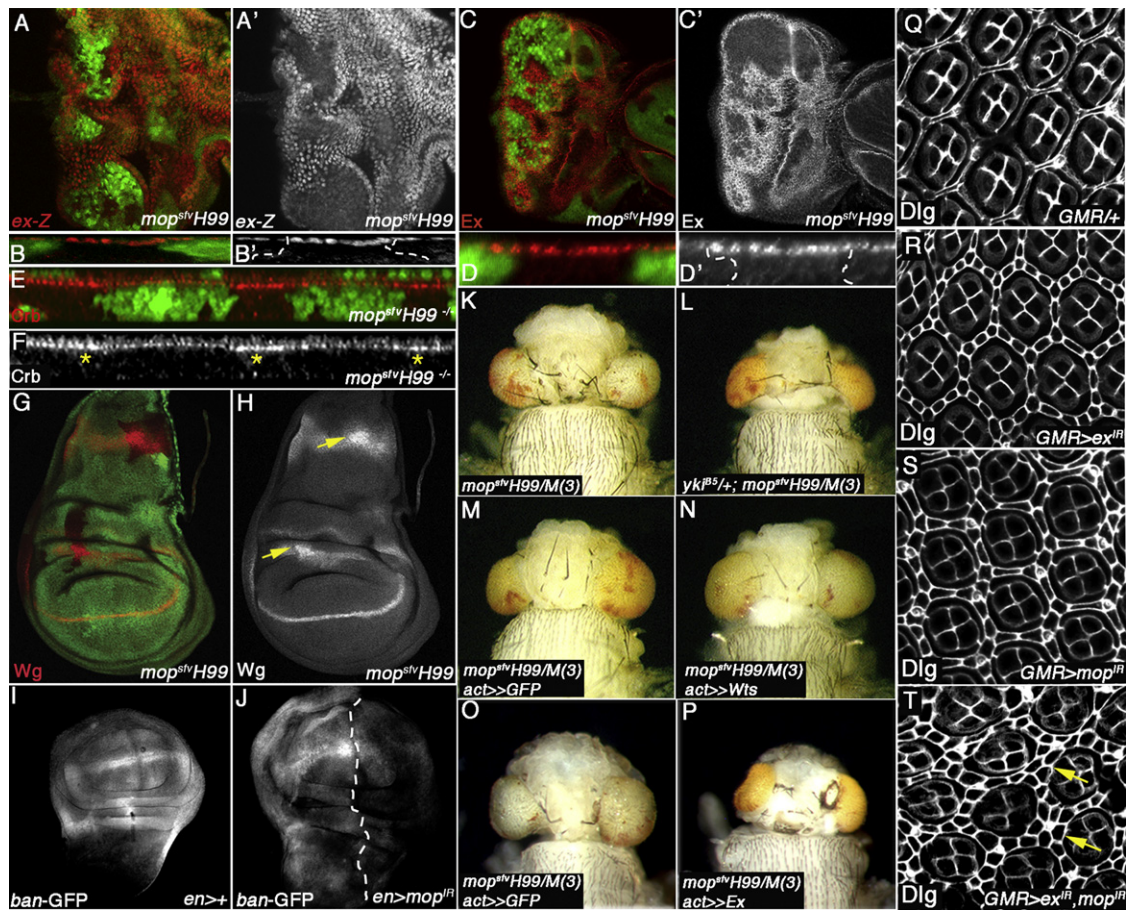
Figure 4. *mop* Promotes SWH Signaling and Is Epistatic to *warts*

(A–H) Confocal images of *mop^sfvH99* clones (marked by the absence of GFP) in the larval eye (A–F) or wing (G and H) analyzed for expression of *ex-lacZ* (*ex-Z*) (optical section in A and A′ and transverse section in B and B′), Ex (optical section in C and C′ and transverse section in D and D′), Crb (transverse section in E and F), or Wg (G and H). Stars in (F) denote increased apical Crb in *mop^sfvH99* clones. Arrows in (H) denote increased Wg protein in *mop^sfvH99* clones in the proximal wing and the notum.

(I and J) Confocal images of *bantam* activity (visualized by *ban*-GFP) in control *en > Gal4* (I) and *en > Gal4,mop^IR* (J) discs. Dashed line denotes A:P boundary.

(K–P) Bright-field images of *mop^sfvH99/M(3)* control heads (K, M, and O) and *mop^sfvH99/M(3)* heads that are either heterozygous for the *yki^B5* allele (L), expressing *UAS-Wts* (N), or *UAS-Expanded* (full-length) (P). The *yki^B5*/+ experiment was carried out with the *mop^sfv11* allele.

(Q–T) Confocal images of control *GMR/+* (Q), *GMR > ex^IR* (R), *GMR > mop^IR* (S), and *GMR > ex^IR,mop^IR* (T) 48 hr APF pupal eye discs stained with Dlg (white). Yellow arrows in (T) denote multilayered interommatidial cells in the *ex^IR, mop^IR* double mutant.

mirrors other peripheral regulators of the SWH pathway, which show mild IOC phenotypes when lost individually, but synergistic effects when combined (e.g., Baumgartner et al., 2010; Genevet et al., 2010; Ling et al., 2010; Yu et al., 2010).

Mop Interacts with Yki via Residues in the Yki WW Domains

To identify the protein target of Mop within the SWH pathway, we undertook an affinity purification/mass spectrometry (AP/MS) analysis of Mop-containing complexes (Kyriakakis et al., 2008; Veraksa et al., 2005) purified from cultured S2 cells. A form of Mop with a point mutation in the putative PTPase catalytic domain (C1728 to alanine; Mop^CS) was used for this analysis in order to enhance interactions with endogenous proteins. This technique identified 14 partially overlapping peptides derived from the endogenous Yki protein (bolded in Figure 5A). Coimmunoprecipitation (coIP) analysis from S2 cells expressing HA-Yki and Mop-V5

confirmed the interaction in the reciprocal orientation: HA-Yki is able to efficiently coIP both Mop^CS and wild-type Mop (Mop^WT) (Figures 5B and 5C). To study the Mop:Yki interaction further, two conserved tyrosines (Y281 and Y350) within the Yki WW domains (see Figure 5A) were individually altered to alanine (A) (HA-Yki^Y281A and HA-Yki^Y350A). Mutation of an equivalent Y residue within the WW domain of polyglutamine tract-binding protein-1 (PQBP1) disrupts binding to PPxY-containing peptides (Tapia et al., 2010). Although expressed at similar levels to HA-Yki, both of the Y-to-A WW mutants are defective in binding to Mop^WT and Mop^CS (Figures 5B and 5C). Mop contains two candidate PPxY motifs located in its linker region between the Bro1 domain and the PTPase-like domain (Figure 5D), indicating that Mop may bind Yki via a WW:PPxY interaction module similar to the interaction between the Yki WW domains and PPxY motifs in Ex, Hpo, and Wts (Badouel et al., 2009; Oh et al., 2009). To test this, each of the Mop PPxY motifs were changed to PPxA
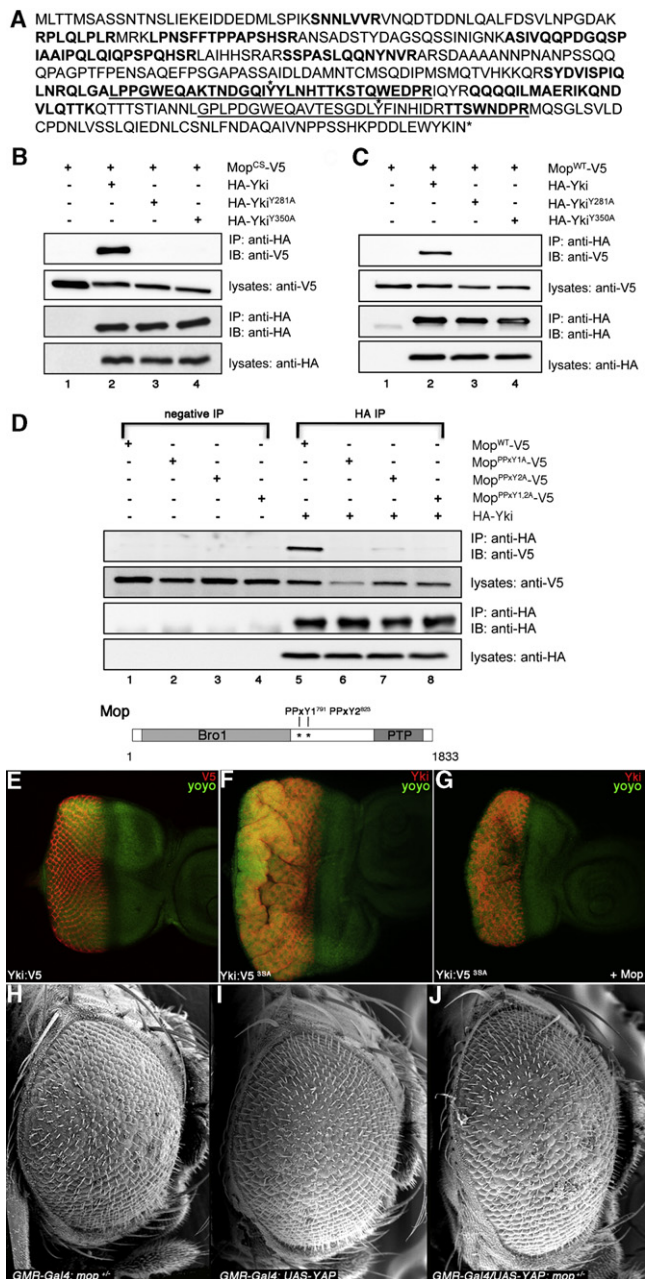
Figure 5. Mop Physically Interacts with Yki via a WW:PPxY Mechanism

(A) The Yki-PF isoform. Fourteen distinct, partially overlapping peptides (indicated in bold) were recovered from affinity purification/mass spectrometry analysis of Mop^{CS}-containing complexes. The WW domains of Yki are underlined, and asterisks denote the conserved tyrosine residues required for the Mop:Yki interaction (see below).

(B) Physical association between Mop^{CS} and Yki. Lanes 1–4: S2 cell lysates expressing the indicated combination of Mop^{CS}-V5 and HA-Yki constructs were immunoprecipitated and probed with the indicated antibodies.

(C) Physical association between Mop^{WT} and Yki. Lanes 1–4: S2 cell lysates expressing the indicated combination of Mop^{WT}-V5 and HA-Yki constructs were immunoprecipitated and probed with the indicated antibodies.

(D) Physical association between Mop^{PPxY} mutants and wild-type Yki. Lanes 1–4: negative control IPs of S2 cell lysates expressing the indicated Mop-V5 constructs. Lanes 5–8: S2 cell lysates expressing the indicated combination of

(PPxY1A, PPxY2A, or PPxY1,2A) and tested for Yki binding. The Mop-PPxY1,2A mutant showed a loss of Yki binding, while each single mutant showed minor residual binding (Figure 5D and data not shown). Thus, Mop can bind to Yki via a WW:PPxY interaction mechanism that is conserved in other SWH proteins that bind directly to Yki.

Mop Inhibition of Yki Is Phosphorylation Independent

A version of Yki carrying serine-to-alanine mutations in three Wts phosphorylation sites (S111A, S168A, and S250A; *UAS-yki:V5^{S3A}*) shows enhanced oncogenic activity due to a loss of inhibitory phosphorylation by Wts (Oh and Irvine, 2009). However, expression of Hpo, Wts, or Ex, which directly bind the Yki WW domains via their PPxY motifs, are able to suppress Yki^{S3A} phenotypes (Oh et al., 2009). To test whether Mop can also regulate Yki in a phosphorylation-independent manner, *UAS-yki:V5* or *UAS-yki:V5^{S3A}* was coexpressed with Mop (*UAS-mop*) in the larval eye. As reported, Yki:V5 shows little effect on growth of the larval eye disc while Yki:V5^{S3A} produces enlarged disc with folds of excess tissue (Figures 5E and 5F). Expression of Mop resulted in substantial suppression of the Yki:V5^{S3A} growth phenotype (Figure 5G). This ability of Mop to antagonize a form of Yki that is refractory to SWH-mediated phosphorylation is consistent with a model in which Mop inhibits Yki directly via the WW:PPxY interaction. Significantly, heterozygosity for *mop* enhances the progrowth effect of the human Yki homolog Yap in the developing eye (Figures 5H–5J), suggesting that the functional relationship between Yki and Mop-like proteins may be conserved.

mop Regulates Association of Yki with Endosomal Compartments

Studies with HD-PTP indicate that the Mop N-terminal Bro1 domain may facilitate interactions with ESCRT endosomal complexes (Doyotte et al., 2008; Ichioka et al., 2007; Odorizzi et al., 2003) and that this underlies the ability of Mop to promote signaling by the EGF and Toll receptors (Huang et al., 2010; Miura et al., 2008). The finding that Mop sequences outside the Bro1 domain bind Yki suggests that Mop may regulate the association of Yki with specific endosome-associated protein complexes, or that Mop physically links Yki to the endosomal trafficking of a receptor-like SWH component such as Fat (for review, see Reddy and Irvine, 2008). To test whether the *mop^{sfvH99}* growth phenotype requires signaling downstream of Fat, we expressed an RNAi knockdown transgene to *approximated* (*app*), which is required for the overgrowth of mutant *fat* tissue (Matakatsu and Blair, 2008), in the *mop^{sfv}H99/M(3)*

wild-type Yki and Mop-V5 constructs were precipitated and probed with the indicated antibodies. A diagram of the Mop protein shows the location of the two PPxY1^{791} and PPxY2^{823} sites.

(E–G) Phosphorylation-independent repression of Yki-driven overgrowth by Mop. Confocal sections of eye imaginal discs expressing *GMR-Gal4, UAS-Yki:V5* (E), *GMR-Gal4, UAS-Yki:V5^{3SA}* (F), *GMR-Gal4, UAS-Yki:V5^{3SA} + UAS-Mop* (G), and stained for V5 (red in E) or Yki (red in F and G) and with nuclei labeled by YOYO-1 iodide (green).

(H–J) YAP-driven overgrowth is sensitive to the genetic dose of *mop*. Scanning electron micrographs (SEM) of *GMR-Gal4, mop-/+* (H), *GMR-Gal4/UAS-YAP* (I), and *GMR-Gal4/UAS-YAP; mop $^{+/-}$* (J) adult eyes.
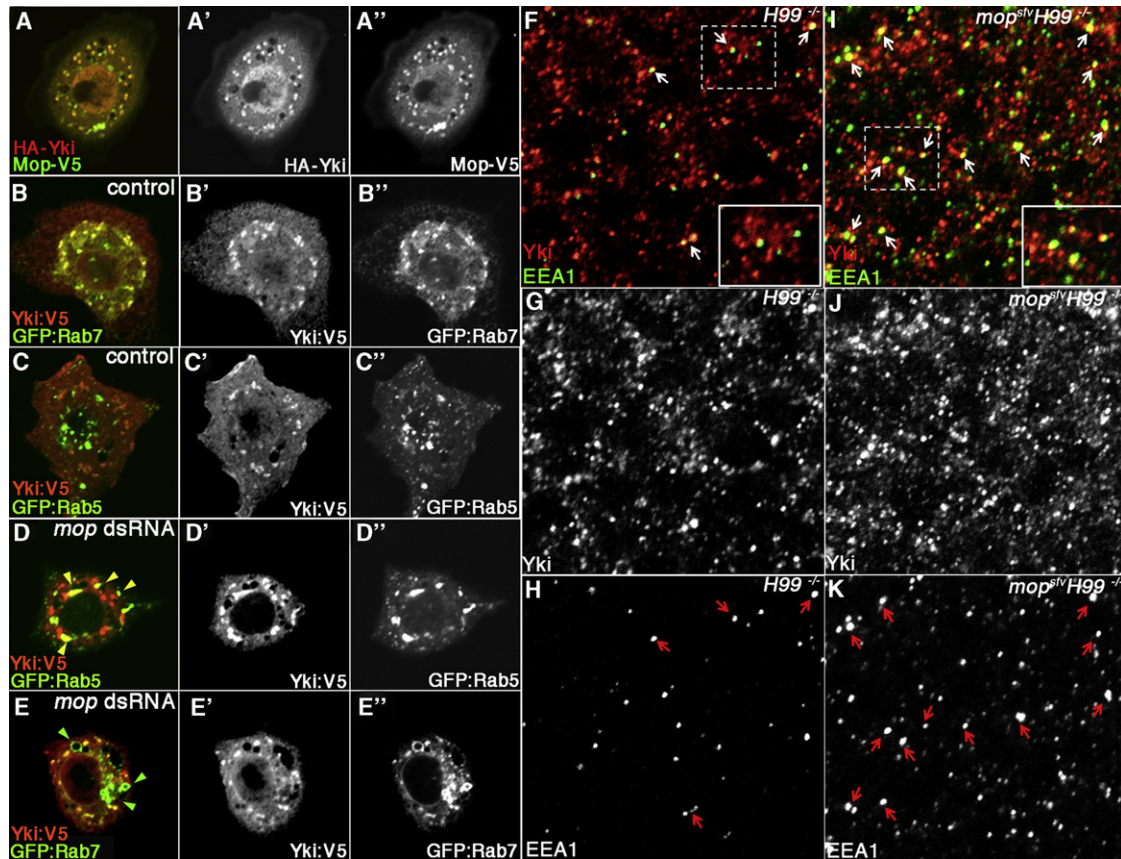
Figure 6. Mop Controls the Endosomal Localization of Yki

(A–C) Confocal images of S2 cells expressing HA-Yki (A and A″ [red]) together with Mop-V5 (A–A″ [green]), or Yki:V5 (B–B″ and C–C″) together with GFP:Rab7 (B–B″) or GFP:Rab5 (C–C″).

(D and E) Confocal images of *mop* dsRNA-treated S2 cells expressing Yki:V5 and either GFP:Rab5 (D–D″) or GFP:Rab7 (E and E′). In *mop* dsRNA-treated S2 cells, a portion of Yki:V5 is relocalized to large Rab5-positive endosomes (yellow arrowheads in D) and is excluded from enlarged Rab7-positive endosomes (green arrowheads in E).

(F–K) Confocal sections of *H99* (F–H) and *mop^{sfv}H99* (I–K) mutant eye imaginal disc tissue, immunostained for endogenous Yki (red) and early endosome antigen-1 (EEA1 [green]). Yki/EEA1 double-positive endosomes are marked by white arrows in (F) and (I) and red arrows in (H) and (K). Red arrows in (K) denote slightly enlarged EEA1 endosomes in *mop,H99* cells that also colocalize with Yki. Dashed boxes correspond to insets. Images were collected at 100× magnification.

background. Knockdown of *app* had no effect on the size of *mop^{sfv}H99/M(3)* heads, and reciprocally, loss of Mop had no discernible effect on Fat levels or the degree of Fat colocalization with the early endosomal marker EEA1 (Figures S2E–S2H), indicating that *mop^{sfv}H99* may promote growth independent of a defect in Fat signaling.

The effect of *mop^{IR}* on Yki protein (see Figures S2I and S2J) led us to examine the relationship between Mop and the cytoplasmic pool of Yki more closely. In imaginal discs and S2 cells, Mop is normally found in cytoplasmic puncta adjacent to Rab5-positive endosomes and partially colocalizes with Rab7-positive endosomes (Huang et al., 2010; Miura et al., 2008). To test whether the physical interaction of Mop and Yki proteins is accompanied by a colocalization of the proteins to specific cytoplasmic structures, HA-Yki and Mop-V5 were visualized in cultured S2 cells. HA-Yki and Mop-V5 substantially colocalize to discrete puncta in the cytoplasm (Figures 6A and 6A″). To identify these Yki-containing structures, Yki:V5 was coexpressed with either GFP-Rab7 or GFP-Rab5 to mark late and early endosomes, respec-

tively. A majority of Yki:V5 protein localizes to Rab7-containing late endosomes in S2 cells (Figures 6B–B″). This parallels the reported partial location of Mop to Rab7 endosomes (Miura et al., 2008) and indicates that Mop and Yki partially colocalize at these structures. By contrast, Yki:V5 is largely excluded from Rab5-containing early endosomes (Figures 6C and 6C″). To test whether depletion of *mop* affects these patterns, Yki:V5 was expressed with either GFP-Rab5 or GFP-Rab7 in cells treated with *mop* dsRNA. As reported (Miura et al., 2008), depletion of *mop* by RNA interference caused an enlargement of GFP-Rab7 endosomes (Figures 6E and 6E″). These enlarged *mop*-knockdown GFP-Rab7 endosomes are depleted for Yki:V5 relative to untreated S2 cells (green arrowheads, Figures 6E and 6E″), and in parallel, Yki:V5 appears in GFP-Rab5 endosomes (yellow arrowheads, Figures 6D and 6D″). This endosomal redistribution of exogenous Yki correlates with an increase in overall levels of the protein and increased expression of the Yki target *ex* as measured by qRT-PCR (Figures S3A and S3C). A similar rise in endogenous Yki levels is observed upon *mop* knockdown in S2
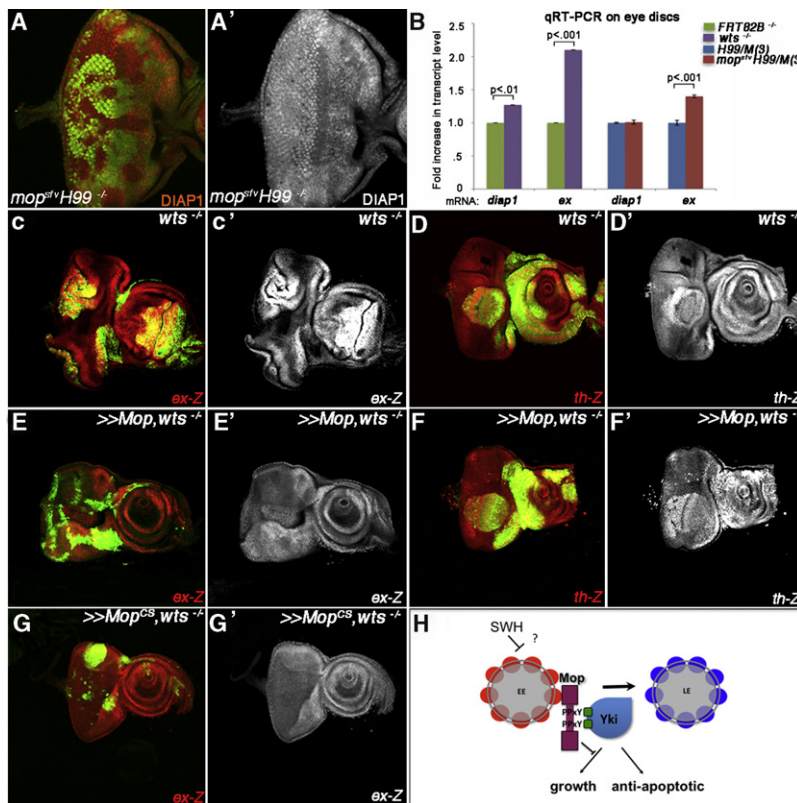
Figure 7. Mop Exhibits Specificity in the Regulation of Yki Activity

(A and A′) Confocal image of a *mop^sfv^H99* mosaic eye disc stained with an antibody to DIAP1.

(B) qRT-PCR analysis of *diap1* and *ex* mRNA levels in *wts* mosaic, *H99/M(3)*, and *mop^sfv^H99/M(3)* eye imaginal discs. P values were calculated using an unpaired t test, and error bars represent standard deviation from the mean of two independent experiments performed in triplicate.

(C–G) Confocal images of *wts* mosaic eye discs (C, C′, D, and D′), or *wts* discs with MARCM-mediated expression of *UAS-Mop* (E, E′, F, and F′) or *UAS-Mop^CS^* (G and G′) stained for expression of *ex-Z* (C, C′, E, E′, G, and G′) or *th-Z* (*diap1*) (D, D′, F, and F′). In all genotypes, *wts* clones are positively marked by GFP (green).

(H) Model of the Mop:Yki interaction. The PPxY motifs in Mop are shown, as are the Yki WW domains (green squares). EE, early endosome; LE, late endosome.

cytoplasmic endogenous Yki (Figures S4D and S4D″). Thus, *mop* loss in imaginal disc tissue leads to an increase in the early-endosome-associated pool of cytoplasmic Yki.

Mop Restricts Ectopic *ex* but Not *diap1* Transcription in Imaginal Discs

Yki lacks DNA binding activity but has been shown to activate transcription of the *diap1* promoter via the DNA binding factor and TEAD homolog Scalloped (Sd) (Goulev et al., 2008; Wu et al., 2008; Zhang et al., 2008). Interestingly, qRT-PCR analysis shows that *mop^sfv^H99* mutant discs elevated expression of *ex* mRNA transcripts but not *diap1* transcripts, while *wts* mutant cells elevated levels of both *ex* and *diap1* transcripts (Figure 7B). In addition, DIAP1 protein is not elevated in *mop^sfv^H99* mutant clones (Figures 7A and 7A′) but is readily detected at elevated levels in *wts* mutant eye disc clones (Figures S4A and S4A′). *diap1-lacZ* (*th-Z*) reporter expression is also unaffected in *mop^sfv^H99* mutant eye clones marked by upregulated Crb (Figures S4B and S4B′). The lack of an effect on *diap1* indicates that Mop may be required to regulate the expression of some SWH targets and not others. To test this, MARCM analysis was used to analyze SWH target gene induction in *wts* mutant clones overexpressing Mop. As previously reported (Hamaratoglu et al., 2006), *ex-Z* and *th-Z* are strongly upregulated in *wts* mutant clones (Figures 7C, 7C′, 7D, and 7D′). Overexpression of wild-type Mop rescues the effect of *wts* loss on *ex-Z* (Figures 7E and 7E′) but does not block elevated *th-Z* expression (Figures 7F and 7F′). The catalytic site mutant form of Mop^CS^ (Miura et al., 2008) was also able to efficiently suppress ectopic *ex-Z* levels in *wts* clones (Figures 7G and 7G′). These data suggest that Mop acts to restrict Yki-driven upregulation of *ex* transcription but not *diap1* transcription and that it does so through a mechanism that does not require Mop catalytic tyrosine phosphatase activity.

DISCUSSION

Here, we describe a screening strategy to identify mutations in *Drosophila* that require a synergistic block in cell death in order

cells, and this correlates with elevated expression of *ex* (Figures S3B and S3C). Moreover, when expressed together with HA-Yki, Mop can retard Yki-driven transcriptional upregulation of *ex* (Figure S3C).

We next examined whether *mop* loss in imaginal disc tissue affects endosomal distribution of endogenous Yki. In control *H99* clones, Yki localizes to punctate cytoplasmic structures that occasionally colocalize with early endosomal antigen-1 (EEA1)-positive early endosomes (Figures 6F–6H). In *mop^sfv^H99* mutant tissue, EEA1-positive endosomes are more abundant and tend to be larger than in control cells (red arrows in Figures 6H and 6K). Yki also accumulates in punctate structures in *mop^sfv^H99* that substantially overlap with enlarged EEA1-positive endosomes (Figures 6I–6K). The extent of Yki:EEA1 colocalization was quantitated by counting the percentage of EEA1-positive endosomes of all sizes that are also positive for Yki. In *H99* control clones, the percentage of EEA1/Yki-positive endosomes is 19% ± 2% (compiled from ten clones containing a total of 380 EEA1-positive endosomes). In *mop^sfv^H99* tissue this approximately doubles to 38% ± 3% (compiled from ten clones containing a total of 584 EEA1-positive endosomes). To determine whether this enrichment of Yki in EEA1 endosomes is accompanied by changes in localization of Yki on late endosomes, the association of Yki with Rab7-positive late endosomes was examined in *H99* and *mop^sfv^H99* clones. In *H99* control clones, Yki localizes to structures that are adjacent to but do not substantially overlap with Rab7 late endosomes (Figures S4E and S4E″). *mop^sfv^H99* clones contain enlarged Rab7-positive endosomes that exclude the increased pool of

to promote tissue overgrowth. Using this approach, we have identified the endosomal protein Mop, which is the *Drosophila* homolog of the candidate mammalian tumor suppressor HD-PTP, as a regulator of the SWH growth inhibitory pathway. Through multiple approaches, we demonstrate that Mop regulates Yki activity via a mechanism involving direct binding and modulation of Yki endosomal association.

This study defines a pool of cytoplasmic Yki that binds Mop and colocalizes with it on endosomes. Data from discs and cultured cells indicate Mop controls endosomal association of this pool of Yki and that a positive correlation exists between Yki colocalization with EEA1-positive early endosomes and Yki levels and activity. A growing body of genetic and molecular data support a role for endosomes as key signaling centers for signal transduction pathways that influence the nuclear translocation of latent cytoplasmic transcription factors (Birtwistle and Kholodenko, 2009; Bokel et al., 2006; Devergne et al., 2007; Di Guglielmo et al., 2003; Fortini and Bilder, 2009) (for review, see Miaczynska et al., 2004; Murphy et al., 2009; Taelman et al., 2010). For example, the activated c-Met receptor associates with the STAT3 transcription factor on EEA1-positive endosomes prior to STAT3 nuclear accumulation, and c-Met delivery to a perinuclear endosomal compartment is necessary to sustain nuclear STAT3 (Kermorgant and Parker, 2008). The enrichment of Yki on EEA1 endosomes and activation of a subset of Yki nuclear targets in *mop* mutant cells suggests that Yki, perhaps in association with receptor complexes, may take a similar route to the nucleus. Intriguingly, microtubule-regulated perinuclear transport of Merlin (Mer) controls nucleocytoplasmic shuttling of Yki (Bensenor et al., 2010). The direct link between Mer transport and Yki shuttling is not clear. However, as Mer can control internalization of transmembrane receptors (for review, see McClatchey and Fehon, 2009), perinuclear transport of Mer might in turn modulate endosomal internalization and transit of Yki:receptor complexes en route to the nucleus.

Genetic data show that exogenous Mop is sufficient to restrict ectopic expression of the Yki-target *ex* but not *diap1* and that loss of endogenous Mop upregulates a set of Yki targets that do not include *diap1*. Mop thus appears to define a regulatory step in determining outputs of the SWH pathway, perhaps as part of the endosomal sorting process. Trafficking of transmembrane proteins down alternate endosomal routes contributes to the activation of different nuclear programs in the Notch, Jak/STAT, and Akt pathways (Hori et al., 2004; Kermorgant and Parker, 2008; Schenck et al., 2008). Similarly, association of Yki-containing complexes with different endosomal compartments may shift Yki nuclear output, perhaps by bringing Yki into contact with posttranslational modifiers or binding partners that affect its ability to activate its suite of target promoters. Further studies will be required to establish whether loss of Mop indeed alters Yki posttranslational modification or the assembly of Yki transcriptional complexes.

In the context of SWH signaling, the differential effect of *mop* loss on *ex* and *diap1* expression place Mop within the growth regulatory arm of the SWH network. Differential effects on the growth and apoptotic outputs of the SWH pathway is also a feature of mutations in *ex* and *mer*, which preferentially drive Yki-dependent clonal growth or antiapoptotic signals, respectively (Pellock et al., 2007) and whose combined mutant phenotypes are more severe than those of single mutants (Hamaratoglu et al., 2006; Maitra et al., 2006). The synergy between *ex* and *mop* alleles on IOC number extends this model and supports the hypothesis that Ex is downstream of *wts* in growth control but upstream of *wts* in apoptotic control (Badouel et al., 2009; Hamaratoglu et al., 2006).

mop mutant cells undergo high rates of caspase-dependent apoptosis in developing eye and wing imaginal discs (this study and Miura et al., 2008). It is probable that this apoptosis is not caused by an effect on *diap1* expression but rather a requirement for Mop in additional prosurvival mechanisms. Knockdown of vertebrate *HD-PTP/PTPN23* elevates levels of tyrosine phosphorylated *f*ocal *a*dhesion *k*inase (FAK) (Castiglioni et al., 2007), which is implicated in cell migration and integrin-mediated survival signals (Mitra and Schlaepfer, 2006). Mop facilitates trafficking of the EGFR receptor into late endosomal compartments and promotes Ras/MAPK signaling downstream of EGFR in the developing retina (Miura et al., 2008). Because the Ras/MAPK module is required to restrain cell death pathways (e.g., Bergmann et al., 1998; Kurada and White, 1998), reduced EGFR-dependent signaling seems likely to contribute to a subset of the apoptotic phenotype of *mop* mutant cells.

The Mop:Yki interaction involves a WW:PPxY interaction mechanism shared by the SWH proteins Ex, Wts, and Hpo that can bind Yki directly and regulate its activity independent of S168 phosphorylation status (Badouel et al., 2009; Oh et al., 2009). Mop represses growth driven by the Yki^{S3A} mutant, indicating that its repressive mechanism is not dependent on Wts kinase activity. As Mop controls the distribution of Yki across endosomal compartments, the paired Bro1 and PPxY domains in Mop could function as a bridge between Yki-containing SWH signaling complexes in the cytoplasm and complexes on the outer membrane of endosomes such as ESCRTs. These complexes could be fairly static or they could assemble and disassemble in response to specific signals. The fact that Mop, Ex, Hpo, and Wts share a WW:PPxY binding mechanism suggests these proteins might compete for Yki binding in the cytosol, or that Mop acts as an endocytic scaffolding factor in a "hand-off" mechanism from the upstream components Ex, Hpo, and Wts. Indeed, understanding the dynamics and composition of the Mop:Yki complex is a significant question going forward. Intriguingly, loss of the Lgl kinase, which regulates cell polarity and membrane compartmentalization (Bilder, 2004), elevates Yki activity by mislocalizing Hpo and the SWH component RASSF in the cytoplasm of disc cells (Grzeschik et al., 2010), suggesting that Hpo and RASSF proteins participate in dynamic and localized interactions in the cytoplasm that are important for their Yki-regulatory function.

The human *HD-PTP/PTPN23* gene resides in a region of the genome (3p21.3) associated with loss of heterozygosity (LOH) in greater than 90% of small cell (SCLC) and non-small-cell (NSCLC) lung cancers (Braga et al., 2002; Kok et al., 1997; Szeles et al., 1997; Toyooka et al., 2000). Yap protein is predominantly nuclear in a subset of primary NSCLC samples and promotes cell proliferation and invasion in NSCLC cell lines, and its expression correlates with poor prognosis in NSCLC patients (Wang et al., 2010). Thus, mutations that deregulate Yap levels and activity are predicted to promote the inappropriate growth and invasiveness of lung epithelial cells. The

mechanism of growth suppression by HD-PTP is not known, but its ability to suppress colony formation of human renal cancer cells is independent of catalytic PTPase activity (Gingras et al., 2009) in much the same way that regulation of Yki by Mop does not require PTPase activity. Although HD-PTP lacks a canonical PPxY motif, genetic data indicate that Mop retains the ability to inhibit Yap activity in the *Drosophila* eye. The extent to which HD-PTP binds Yap or Taz has yet to be examined, but if the relationship between the orthologous *Drosophila* proteins is conserved in vertebrates, this link to Yki/Yap may contribute to growth regulatory roles of vertebrate HD-PTP proteins in development and disease.

EXPERIMENTAL PROCEDURES

Drosophila Genetics

Alleles used: ex^{697} (*ex-Z*) (Boedigheimer et al., 1993), th^{j5c8} (*th-Z*) (Hay et al., 1995), yki^{B5} (Huang et al., 2005), wts^{X1} (Xu et al., 1995), and *H99* (White et al., 1994). Transgenes used: *UAS-Myc-Wts1* (Jia et al., 2003), *UAS-Ex* (Boedigheimer et al., 1997), *UAS-Mop* and *UAS-Mop^{CS}* (Miura et al., 2008), *UAS-Yki:V5* (Oh and Irvine, 2009), *UAS-mop^{IR}* (Vienna *Drosophila* RNAi Collection), and *bantam-GFP* (Brennecke et al., 2003).

Immunofluorescence

Imaginal discs and S2 cells were fixed and stained following standard procedures. Antibodies used: mouse anti-Dlg (1:20, DSHB), mouse anti-BrdU (1:50, Becton Dickinson), mouse anti-cyclin E (1:5, H. Richardson), mouse anti-cyclin A (1:200, DSHB), guinea pig anti-Expanded (1:10,000, R. Fehon), rat anti-Crb (1:500, U. Tepass), mouse anti-Wg (1:800, DSHB), mouse anti-β-galactosidase (1:1000, Promega), mouse anti-V5 (1:200, Invitrogen) and mouse anti-HA High Affinity (1:100, Roche), mouse anti-Yki (1:100, Zhi-Chun Lai), rabbit anti-EEA1 (1:250, Thermo-Scientific), and mouse anti-DIAP1 (1:400, B. Hay).

Clonal Cell Counts and Cell-Cycle Analysis

For FACS analysis, *H99/M(3)* and *mop^{sfv}H99/M(3)* wing discs were dissociated in PBS Trypsin-EDTA and stained with 20 μM DRAQ-5 (Biostatus Limited). Data were acquired on a Becton Dickinson LSR II flow cytometer and analyzed with FlowJo Software. Clonal cell count data were generated by producing heat-shocked *H99* and *mop^{sfv}H99* wing clones 48 hr AED. At 96 AED, wing discs were fixed and stained with DRAQ5, and the number of nuclei per clone and twin-spot pair was counted.

Quantitative RT-PCR

Total RNA was extracted from larval eye discs using TRizol (Invitrogen) and purified using RNeasy Mini Kit (QIAGEN). Superscript II RT and random primers (Invitrogen) were used to produce cDNAs. Exon-specific primers were used with SYBR Green I Master (Roche) to perform qPCR reactions using a Roche LightCycler 480. All reactions were performed in triplicate, and the relative amount of *diap1* and *ex* mRNA was normalized to *β-tubulin* transcript.

Cell Culture

Drosophila S2 cells were maintained at 25°C in Schneider's *Drosophila* medium (GIBCO) supplemented with 10% heat-inactivated fetal bovine serum (GIBCO). Proteins were induced with 0.35 mM CuSO$_4$ overnight. To establish a stable cell line of pMK33-GSNTAP-Mop^{CS}, S2 cells were transfected using Effectene transfection reagent (QIAGEN). After 48 hr of incubation with the transfection reagent, cells were maintained in complete media with 300 μg/ml hygromycin (Sigma). *mop* dsRNA was generated using the T7 Ribo-MAX system (Promega) using the following primers: 5′-T7-TGCCCACATTA CCGAGTTATCG-3′ and 5′-T7-TTTCCGCTATTGGTTTGCTGAC-3′. *mop* dsRNA was transfected into cells using Cellfectin (Invitrogen), and cells were incubated for 48 hr, followed by transfection with the following constructs: (1) *pAc5.1-Yki:V5*, (2) *UAS-GFP:Rab5*, (3) *UAS-GFP:Rab7*, (4) *pMT-Gal4*, followed by another 48 hr incubation and induction with 0.5 mM CuSO$_4$ for 4 hr.

Immunoprecipitation

Cell extracts were lysed in lysis buffer (LB: 50 mM Tris [pH 7.5], 125 mM NaCl, 5% glycerol, 0.2% IGEPAL, 1.5 mM MgCl$_2$, 1 mM DTT, 25 mM NaF, 1 mM Na$_3$VO$_4$, 1 mM EDTA, and complete protease inhibitor [Roche]), and lysates were incubated with anti-HA affinity beads (Sigma) for 2 hr at 4°C, followed by extensive washes. Protein complexes were eluted with SDS sample buffer, separated on SDS protein gels, transferred onto Immun-Blot PVDF membranes (Bio-Rad), and probed with mouse anti-HA or mouse anti-V5 antibodies (Sigma).

SUPPLEMENTAL INFORMATION

Supplemental Information includes Supplemental Experimental Procedures, Supplemental References, and four figures and can be found with this article online at doi:10.1016/j.devcel.2011.04.012.

REFERENCES

Asano, M., Nevins, J.R., and Wharton, R.P. (1996). Ectopic E2F expression induces S phase and apoptosis in Drosophila imaginal discs. Genes Dev. 10, 1422–1432.

Badouel, C., Gardano, L., Amin, N., Garg, A., Rosenfeld, R., Le Bihan, T., and McNeill, H. (2009). The FERM-domain protein Expanded regulates Hippo pathway activity via direct interactions with the transcriptional activator Yorkie. Dev. Cell 16, 411–420.

Baumgartner, R., Poernbacher, I., Buser, N., Hafen, E., and Stocker, H. (2010). The WW domain protein Kibra acts upstream of Hippo in Drosophila. Dev. Cell 18, 309–316.

Bennett, F.C., and Harvey, K.F. (2006). Fat cadherin modulates organ size in Drosophila via the Salvador/Warts/Hippo signaling pathway. Curr. Biol. 16, 2101–2110.

Bensenor, L.B., Barlan, K., Rice, S.E., Fehon, R.G., and Gelfand, V.I. (2010). Microtubule-mediated transport of the tumor-suppressor protein Merlin and its mutants. Proc. Natl. Acad. Sci. USA 107, 7311–7316.

Bergmann, A., Agapite, J., McCall, K., and Steller, H. (1998). The Drosophila gene hid is a direct molecular target of Ras-dependent survival signaling. Cell 95, 331–341.

Bilder, D. (2004). Epithelial polarity and proliferation control: links from the Drosophila neoplastic tumor suppressors. Genes Dev. 18, 1909–1925.

Birtwistle, M.R., and Kholodenko, B.N. (2009). Endocytosis and signalling: a meeting with mathematics. Mol. Oncol. 3, 308–320.

Boedigheimer, M., Bryant, P., and Laughon, A. (1993). Expanded, a negative regulator of cell proliferation in Drosophila, shows homology to the NF2 tumor suppressor. Mech. Dev. 44, 83–84.

Boedigheimer, M.J., Nguyen, K.P., and Bryant, P.J. (1997). Expanded functions in the apical cell domain to regulate the growth rate of imaginal discs. Dev. Genet. 20, 103–110.

Bokel, C., Schwabedissen, A., Entchev, E., Renaud, O., and Gonzalez-Gaitan, M. (2006). Sara endosomes and the maintenance of Dpp signaling levels across mitosis. Science 314, 1135–1139.

Braga, E., Senchenko, V., Bazov, I., Loginov, W., Liu, J., Ermilova, V., Kazubskaya, T., Garkavtseva, R., Mazurenko, N., Kisseljov, F., et al. (2002). Critical tumor-suppressor gene regions on chromosome 3P in major human epithelial malignancies: allelotyping and quantitative real-time PCR. Int. J. Cancer 100, 534–541.

Brennecke, J., Hipfner, D.R., Stark, A., Russell, R.B., and Cohen, S.M. (2003). bantam encodes a developmentally regulated microRNA that controls cell proliferation and regulates the proapoptotic gene hid in Drosophila. Cell 113, 25–36.

Brumby, A.M., and Richardson, H.E. (2005). Using Drosophila melanogaster to map human cancer pathways. Nat. Rev. Cancer 5, 626–639.

Castiglioni, S., Maier, J.A., and Mariotti, M. (2007). The tyrosine phosphatase HD-PTP: A novel player in endothelial migration. Biochem. Biophys. Res. Commun. 364, 534–539.

Chen, C.L., Gajewski, K.M., Hamaratoglu, F., Bossuyt, W., Sansores-Garcia, L., Tao, C., and Halder, G. (2010). The apical-basal cell polarity determinant Crumbs regulates Hippo signaling in Drosophila. Proc. Natl. Acad. Sci. USA 107, 15810–15815.

Chi, C., Zhu, H., Han, M., Zhuang, Y., Wu, X., and Xu, T. (2010). Disruption of lysosome function promotes tumor growth and metastasis in Drosophila. J. Biol. Chem. 285, 21817–21823.

Cho, E., Feng, Y., Rauskolb, C., Maitra, S., Fehon, R., and Irvine, K.D. (2006). Delineation of a Fat tumor suppressor pathway. Nat. Genet. 38, 1142–1150.

Devergne, O., Ghiglione, C., and Noselli, S. (2007). The endocytic control of JAK/STAT signalling in Drosophila. J. Cell Sci. 120, 3457–3464.

Di Guglielmo, G.M., Le Roy, C., Goodfellow, A.F., and Wrana, J.L. (2003). Distinct endocytic pathways regulate TGF-beta receptor signalling and turnover. Nat. Cell Biol. 5, 410–421.

Dong, J., Feldmann, G., Huang, J., Wu, S., Zhang, N., Comerford, S.A., Gayyed, M.F., Anders, R.A., Maitra, A., and Pan, D. (2007). Elucidation of a universal size-control mechanism in Drosophila and mammals. Cell 130, 1120–1133.

Doyotte, A., Mironov, A., McKenzie, E., and Woodman, P. (2008). The Bro1-related protein HD-PTP/PTPN23 is required for endosomal cargo sorting and multivesicular body morphogenesis. Proc. Natl. Acad. Sci. USA 105, 6308–6313.

Evan, G.I., and Vousden, K.H. (2001). Proliferation, cell cycle and apoptosis in cancer. Nature 411, 342–348.

Fortini, M.E., and Bilder, D. (2009). Endocytic regulation of Notch signaling. Curr. Opin. Genet. Dev. 19, 323–328.

Genevet, A., Polesello, C., Blight, K., Robertson, F., Collinson, L.M., Pichaud, F., and Tapon, N. (2009). The Hippo pathway regulates apical-domain size independently of its growth-control function. J. Cell Sci. 122, 2360–2370.

Genevet, A., Wehr, M.C., Brain, R., Thompson, B.J., and Tapon, N. (2010). Kibra is a regulator of the Salvador/Warts/Hippo signaling network. Dev. Cell 18, 300–308.

Gingras, M.C., Zhang, Y.L., Kharitidi, D., Barr, A.J., Knapp, S., Tremblay, M.L., and Pause, A. (2009). HD-PTP is a catalytically inactive tyrosine phosphatase due to a conserved divergence in its phosphatase domain. PLoS ONE 4, e5105.

Goulev, Y., Fauny, J.D., Gonzalez-Marti, B., Flagiello, D., Silber, J., and Zider, A. (2008). SCALLOPED interacts with YORKIE, the nuclear effector of the hippo tumor-suppressor pathway in Drosophila. Curr. Biol. 18, 435–441.

Grzeschik, N.A., Parsons, L.M., Allott, M.L., Harvey, K.F., and Richardson, H.E. (2010). Lgl, aPKC, and Crumbs regulate the Salvador/Warts/Hippo pathway through two distinct mechanisms. Curr. Biol. 20, 573–581.

Halder, G., and Johnson, R.L. (2011). Hippo signaling: growth control and beyond. Development 138, 9–22.

Hamaratoglu, F., Willecke, M., Kango-Singh, M., Nolo, R., Hyun, E., Tao, C., Jafar-Nejad, H., and Halder, G. (2006). The tumour-suppressor genes NF2/Merlin and Expanded act through Hippo signalling to regulate cell proliferation and apoptosis. Nat. Cell Biol. 8, 27–36.

Hamaratoglu, F., Gajewski, K., Sansores-Garcia, L., Morrison, C., Tao, C., and Halder, G. (2009). The Hippo tumor-suppressor pathway regulates apical-domain size in parallel to tissue growth. J. Cell Sci. 122, 2351–2359.

Harvey, K.F., Pfleger, C.M., and Hariharan, I.K. (2003). The Drosophila Mst ortholog, hippo, restricts growth and cell proliferation and promotes apoptosis. Cell 114, 457–467.

Hay, B.A., Wassarman, D.A., and Rubin, G.M. (1995). Drosophila homologs of baculovirus inhibitor of apoptosis proteins function to block cell death. Cell 83, 1253–1262.

Hori, K., Fostier, M., Ito, M., Fuwa, T.J., Go, M.J., Okano, H., Baron, M., and Matsuno, K. (2004). Drosophila deltex mediates suppressor of Hairless-independent and late-endosomal activation of Notch signaling. Development 131, 5527–5537.

Huang, J., Wu, S., Barrera, J., Matthews, K., and Pan, D. (2005). The Hippo signaling pathway coordinately regulates cell proliferation and apoptosis by inactivating Yorkie, the Drosophila Homolog of YAP. Cell 122, 421–434.

Huang, H.R., Chen, Z.J., Kunes, S., Chang, G.D., and Maniatis, T. (2010). Endocytic pathway is required for Drosophila Toll innate immune signaling. Proc. Natl. Acad. Sci. USA 107, 8322–8327.

Ichioka, F., Takaya, E., Suzuki, H., Kajigaya, S., Buchman, V.L., Shibata, H., and Maki, M. (2007). HD-PTP and Alix share some membrane-traffic related proteins that interact with their Bro1 domains or proline-rich regions. Arch. Biochem. Biophys. 457, 142–149.

Jia, J., Zhang, W., Wang, B., Trinko, R., and Jiang, J. (2003). The Drosophila Ste20 family kinase dMST functions as a tumor suppressor by restricting cell proliferation and promoting apoptosis. Genes Dev. 17, 2514–2519.

Justice, R.W., Zilian, O., Woods, D.F., Noll, M., and Bryant, P.J. (1995). The Drosophila tumor suppressor gene warts encodes a homolog of human myotonic dystrophy kinase and is required for the control of cell shape and proliferation. Genes Dev. 9, 534–546.

Kango-Singh, M., Nolo, R., Tao, C., Verstreken, P., Hiesinger, P.R., Bellen, H.J., and Halder, G. (2002). Shar-pei mediates cell proliferation arrest during imaginal disc growth in Drosophila. Development 129, 5719–5730.

Kermorgant, S., and Parker, P.J. (2008). Receptor trafficking controls weak signal delivery: a strategy used by c-Met for STAT3 nuclear accumulation. J. Cell Biol. 182, 855–863.

Kim, J., Sitaraman, S., Hierro, A., Beach, B.M., Odorizzi, G., and Hurley, J.H. (2005). Structural basis for endosomal targeting by the Bro1 domain. Dev. Cell 8, 937–947.

Kok, K., Naylor, S.L., and Buys, C.H. (1997). Deletions of the short arm of chromosome 3 in solid tumors and the search for suppressor genes. Adv. Cancer Res. 71, 27–92.

Kurada, P., and White, K. (1998). Ras promotes cell survival in Drosophila by downregulating hid expression. Cell 95, 319–329.

Kyriakakis, P., Tipping, M., Abed, L., and Veraksa, A. (2008). Tandem affinity purification in Drosophila: the advantages of the GS-TAP system. Fly (Austin) 2, 229–235.

Lai, Z.C., Wei, X., Shimizu, T., Ramos, E., Rohrbaugh, M., Nikolaidis, N., Ho, L.L., and Li, Y. (2005). Control of cell proliferation and apoptosis by mob as tumor suppressor, mats. Cell 120, 675–685.

Levy, D., Adamovich, Y., Reuven, N., and Shaul, Y. (2008). Yap1 phosphorylation by c-Abl is a critical step in selective activation of proapoptotic genes in response to DNA damage. Mol. Cell 29, 350–361.

Ling, C., Zheng, Y., Yin, F., Yu, J., Huang, J., Hong, Y., Wu, S., and Pan, D. (2010). The apical transmembrane protein Crumbs functions as a tumor suppressor that regulates Hippo signaling by binding to Expanded. Proc. Natl. Acad. Sci. USA 107, 10532–10537.

Maitra, S., Kulikauskas, R.M., Gavilan, H., and Fehon, R.G. (2006). The tumor suppressors Merlin and Expanded function cooperatively to modulate receptor endocytosis and signaling. Curr. Biol. 16, 702–709.

Matakatsu, H., and Blair, S.S. (2008). The DHHC palmitoyltransferase approximated regulates Fat signaling and Dachs localization and activity. Curr. Biol. *18*, 1390–1395.

McClatchey, A.I., and Fehon, R.G. (2009). Merlin and the ERM proteins–regulators of receptor distribution and signaling at the cell cortex. Trends Cell Biol. *19*, 198–206.

Miaczynska, M., Pelkmans, L., and Zerial, M. (2004). Not just a sink: endosomes in control of signal transduction. Curr. Opin. Cell Biol. *16*, 400–406.

Mitra, S.K., and Schlaepfer, D.D. (2006). Integrin-regulated FAK-Src signaling in normal and cancer cells. Curr. Opin. Cell Biol. *18*, 516–523.

Miura, G.I., Roignant, J.Y., Wassef, M., and Treisman, J.E. (2008). Myopic acts in the endocytic pathway to enhance signaling by the Drosophila EGF receptor. Development *135*, 1913–1922.

Murphy, J.E., Padilla, B.E., Hasdemir, B., Cottrell, G.S., and Bunnett, N.W. (2009). Endosomes: a legitimate platform for the signaling train. Proc. Natl. Acad. Sci. USA *106*, 17615–17622.

Newsome, T.P., Asling, B., and Dickson, B.J. (2000). Analysis of Drosophila photoreceptor axon guidance in eye-specific mosaics. Development *127*, 851–860.

Nicholson, S.C., Gilbert, M.M., Nicolay, B.N., Frolov, M.V., and Moberg, K.H. (2009). The archipelago tumor suppressor gene limits Rb/E2F-regulated apoptosis in developing drosophila tissues. Curr. Biol. *19*, 1503–1510.

Odorizzi, G., Katzmann, D.J., Babst, M., Audhya, A., and Emr, S.D. (2003). Bro1 is an endosome-associated protein that functions in the MVB pathway in Saccharomyces cerevisiae. J. Cell Sci. *116*, 1893–1903.

Oh, H., and Irvine, K.D. (2008). In vivo regulation of Yorkie phosphorylation and localization. Development *135*, 1081–1088.

Oh, H., and Irvine, K.D. (2009). In vivo analysis of Yorkie phosphorylation sites. Oncogene *28*, 1916–1927.

Oh, H., and Irvine, K.D. (2011). Cooperative regulation of growth by Yorkie and Mad through bantam. Dev. Cell *20*, 109–122.

Oh, H., Reddy, B.V., and Irvine, K.D. (2009). Phosphorylation-independent repression of Yorkie in Fat-Hippo signaling. Dev. Biol. *335*, 188–197.

Pagliarini, R.A., and Xu, T. (2003). A genetic screen in Drosophila for metastatic behavior. Science *302*, 1227–1231.

Pan, D. (2010). The hippo signaling pathway in development and cancer. Dev. Cell *19*, 491–505.

Pantalacci, S., Tapon, N., and Leopold, P. (2003). The Salvador partner Hippo promotes apoptosis and cell-cycle exit in Drosophila. Nat. Cell Biol. *5*, 921–927.

Pellock, B.J., Buff, E., White, K., and Hariharan, I.K. (2007). The Drosophila tumor suppressors Expanded and Merlin differentially regulate cell cycle exit, apoptosis, and Wingless signaling. Dev. Biol. *304*, 102–115.

Peng, H.W., Slattery, M., and Mann, R.S. (2009). Transcription factor choice in the Hippo signaling pathway: homothorax and yorkie regulation of the microRNA bantam in the progenitor domain of the Drosophila eye imaginal disc. Genes Dev. *23*, 2307–2319.

Reddy, B.V., and Irvine, K.D. (2008). The Fat and Warts signaling pathways: new insights into their regulation, mechanism and conservation. Development *135*, 2827–2838.

Ren, F., Zhang, L., and Jiang, J. (2010). Hippo signaling regulates Yorkie nuclear localization and activity through 14-3-3 dependent and independent mechanisms. Dev. Biol. *337*, 303–312.

Robinson, B.S., Huang, J., Hong, Y., and Moberg, K.H. (2010). Crumbs regulates Salvador/Warts/Hippo signaling in Drosophila via the FERM-domain protein expanded. Curr. Biol. *20*, 582–590.

Schenck, A., Goto-Silva, L., Collinet, C., Rhinn, M., Giner, A., Habermann, B., Brand, M., and Zerial, M. (2008). The endosomal protein Appl1 mediates Akt substrate specificity and cell survival in vertebrate development. Cell *133*, 486–497.

Silva, E., Tsatskis, Y., Gardano, L., Tapon, N., and McNeill, H. (2006). The tumor-suppressor gene fat controls tissue growth upstream of expanded in the hippo signaling pathway. Curr. Biol. *16*, 2081–2089.

Staehling-Hampton, K., Ciampa, P.J., Brook, A., and Dyson, N. (1999). A genetic screen for modifiers of E2F in Drosophila melanogaster. Genetics *153*, 275–287.

Strano, S., Monti, O., Pediconi, N., Baccarini, A., Fontemaggi, G., Lapi, E., Mantovani, F., Damalas, A., Citro, G., Sacchi, A., et al. (2005). The transcriptional coactivator Yes-associated protein drives p73 gene-target specificity in response to DNA Damage. Mol. Cell *18*, 447–459.

Szeles, A., Yang, Y., Sandlund, A.M., Kholodnyuk, I., Kiss, H., Kost-Alimova, M., Zabarovsky, E.R., Stanbridge, E., Klein, G., and Imreh, S. (1997). Human/mouse microcell hybrid based elimination test reduces the putative tumor suppressor region at 3p21.3 to 1.6 cM. Genes Chromosomes Cancer *20*, 329–336.

Taelman, V.F., Dobrowolski, R., Plouhinec, J.L., Fuentealba, L.C., Vorwald, P.P., Gumper, I., Sabatini, D.D., and De Robertis, E.M. (2010). Wnt signaling requires sequestration of glycogen synthase kinase 3 inside multivesicular endosomes. Cell *143*, 1136–1148.

Tapia, V.E., Nicolaescu, E., McDonald, C.B., Musi, V., Oka, T., Inayoshi, Y., Satteson, A.C., Mazack, V., Humbert, J., Gaffney, C.J., et al. (2010). Y65C missense mutation in the WW domain of the Golabi-Ito-Hall syndrome protein PQBP1 affects its binding activity and deregulates pre-mRNA splicing. J. Biol. Chem. *285*, 19391–19401.

Tapon, N., Harvey, K.F., Bell, D.W., Wahrer, D.C.R., Schiripo, T.A., Haber, D.A., and Hariharan, I.K. (2002). salvador Promotes Both Cell Cycle Exit and Apoptosis in Drosophila and Is Mutated in Human Cancer Cell Lines. Cell *110*, 467–478.

Toyooka, S., Ouchida, M., Jitsumori, Y., Tsukuda, K., Sakai, A., Nakamura, A., Shimizu, N., and Shimizu, K. (2000). HD-PTP: A novel protein tyrosine phosphatase gene on human chromosome 3p21.3. Biochem. Biophys. Res. Commun. *278*, 671–678.

Udan, R.S., Kango-Singh, M., Nolo, R., Tao, C., and Halder, G. (2003). Hippo promotes proliferation arrest and apoptosis in the Salvador/Warts pathway. Nat. Cell Biol. *5*, 914–920.

Veraksa, A., Bauer, A., and Artavanis-Tsakonas, S. (2005). Analyzing protein complexes in Drosophila with tandem affinity purification-mass spectrometry. Dev. Dyn. *232*, 827–834.

Wang, Y., Dong, Q., Zhang, Q., Li, Z., Wang, E., and Qiu, X. (2010). Overexpression of yes-associated protein contributes to progression and poor prognosis of non-small-cell lung cancer. Cancer Sci. *101*, 1279–1285.

Wei, X., Shimizu, T., and Lai, Z.C. (2007). Mob as tumor suppressor is activated by Hippo kinase for growth inhibition in Drosophila. EMBO J. *26*, 1772–1781.

White, K., Grether, M.E., Abrams, J.M., Young, L., Farrell, K., and Steller, H. (1994). Genetic control of programmed cell death in Drosophila. Science *264*, 677–683.

Willecke, M., Hamaratoglu, F., Kango-Singh, M., Udan, R., Chen, C.L., Tao, C., Zhang, X., and Halder, G. (2006). The fat cadherin acts through the hippo tumor-suppressor pathway to regulate tissue size. Curr. Biol. *16*, 2090–2100.

Wolff, T., and Ready, D.F. (1993). Pattern formation in the *Drosophila* retina. In The Development of *Drosophila melanogaster*, M. Bate and A. Martinez Arias, eds. (Plainview, NY: Cold Spring Harbor Laboratory Press), pp. 1277–1325.

Wu, S., Huang, J., Dong, J., and Pan, D. (2003). hippo encodes a Ste-20 family protein kinase that restricts cell proliferation and promotes apoptosis in conjunction with salvador and warts. Cell *114*, 445–456.

Wu, S., Liu, Y., Zheng, Y., Dong, J., and Pan, D. (2008). The TEAD/TEF family protein Scalloped mediates transcriptional output of the Hippo growth-regulatory pathway. Dev. Cell *14*, 388–398.

Wu, M., Pastor-Pareja, J.C., and Xu, T. (2010). Interaction between Ras(V12) and scribbled clones induces tumour growth and invasion. Nature *463*, 545–548.

Xu, T., Wang, W., Zhang, S., Stewart, R.A., and Yu, W. (1995). Identifying tumor suppressors in genetic mosaics: the Drosophila lats gene encodes a putative protein kinase. Development *121*, 1053–1063.

Yu, J., Zheng, Y., Dong, J., Klusza, S., Deng, W.M., and Pan, D. (2010). Kibra functions as a tumor suppressor protein that regulates Hippo signaling in conjunction with Merlin and Expanded. Dev. Cell *18*, 288–299.

Zaidi, S.K., Sullivan, A.J., Medina, R., Ito, Y., van Wijnen, A.J., Stein, J.L., Lian, J.B., and Stein, G.S. (2004). Tyrosine phosphorylation controls Runx2-mediated subnuclear targeting of YAP to repress transcription. EMBO J. *23*, 790–799.

Zhang, L., Ren, F., Zhang, Q., Chen, Y., Wang, B., and Jiang, J. (2008). The TEAD/TEF family of transcription factor Scalloped mediates Hippo signaling in organ size control. Dev. Cell *14*, 377–387.

Zhao, B., Ye, X., Yu, J., Li, L., Li, W., Li, S., Lin, J.D., Wang, C.Y., Chinnaiyan, A.M., Lai, Z.C., et al. (2008). TEAD mediates YAP-dependent gene induction and growth control. Genes Dev. *22*, 1962–1971.

Zhao, B., Li, L., Lei, Q., and Guan, K.L. (2010). The Hippo-YAP pathway in organ size control and tumorigenesis: an updated version. Genes Dev. *24*, 862–874.